Supplementary material for $\mathcal{PT}$-symmetric Non-Hermitian Hopf Metal

I. BLOCH HAMILTONIAN AND ZAK PHASE

In this section, we discuss Zak phases associated with eigenstates of the non-Hermitian Hamiltonian describing the non-Hermitian Hopf metal.

A. Bloch Hamiltonian

The two-band Bloch Hamiltonian of the $\mathcal{PT}$-symmetric non-Hermitian system can be generally written as,

$$H = n_x(\mathbf{k})\sigma_x + n_z(\mathbf{k})\sigma_z + im_y(\mathbf{k})\sigma_y, \tag{1}$$

here $n_x(\mathbf{k}),\ n_y(\mathbf{k}),\ n_z(\mathbf{k})$ are real parameters as functions of Bloch momenta $\mathbf{k} = (k_x,\ k_y,\ k_z)$. The modified Bloch sphere is represented as the spherical polar coordinates described as follows,

$$n_x = \sin(\theta)\cos(\Phi), \quad n_z = \sin(\theta)\sin(\Phi), \quad m_y = \cos(\theta), \tag{2}$$

where $\theta \in [0, \pi]$ and $\Phi \in [0, 2\pi]$ describe the polar and azimuthal angles, respectively. The eigenvalue equation for the above Hamiltonian is expressed as follows

$$H(\theta, \Phi)|\psi_n(\theta, \Phi)\rangle = E_n(\theta, \Phi)|\psi_n(\theta, \Phi)\rangle. \tag{3}$$

Here $E_n(\theta, \Phi),\ n = 1, 2$ denotes an eigenvalue of $H(\theta, \Phi)$ with corresponding right eigenstate $|\psi_n(\theta, \Phi)\rangle$. In the parameter regime, $\pi/4 \leq \theta \leq 3\pi/4$ with $\Phi \in [0, 2\pi]$, $H(\theta, \Phi)$ has purely real eigenvalues with corresponding real-valued eigenstates (see the left top panel of Fig. 1). Therefore, the parameter regime $\pi/4 \leq \theta \leq 3\pi/4$ with $\Phi \in [0, 2\pi]$ describes the $\mathcal{PT}$-exact phase of the system. Whereas, the parameter regimes $0 < \theta < \pi/4$ and $\pi/4 < \theta < 2\pi$ with $\Phi \in [0, 2\pi]$ describe $\mathcal{PT}$-broken phases of the system where both eigenvalues are purely imaginary (see the left top panel of Fig. 1). The transitions from the $\mathcal{PT}$-exact phase to $\mathcal{PT}$-broken phases accompany exceptional points at $\theta = \pi/4,\ 3\pi/4$, and the collection of exceptional points for all values of Φ defines exceptional rings on the Bloch sphere [See the top left panel and right panel of Fig. 1].

B. Numerical computation of the Zak phase

The Zak phase is the geometric phase associated with the non-degenerate eigenstate $|\psi_n(\xi)\rangle)$ that is accumulated via traversing a 1D closed manifold C in the parameter space and given by [1, 2],

$$\phi_n = \oint_{\mathrm{C}} i\langle\psi_n(\xi)|\nabla_\xi\psi_n(\xi)\rangle \cdot d\xi. \tag{4}$$

Here ξ describes the closed manifolds in the parameter space and can be expressed as a function of the polar angle θ and azimuthal angle Φ on the Bloch sphere. $|\psi_n(\xi)\rangle$ is n-th right eigenstate. Some examples of 1D closed manifolds on the Bloch sphere are $C_{\mathrm{a}},\ C_{\mathrm{b}},\ C_c,\ C_{\mathrm{d}}$ which are shown in the left panel of Fig. 1.

In order to gain some physical insights, we use a systematic formalism of the parallel transport gauge for the numerical computation of Zak phases which we discuss as follows [3–7]. We consider a discrete uniform mesh of ξ points $\{\xi_j,\ j = 1, 2, ..., N, N+1\}$ such that $\xi_{j+1} = \xi_j + \delta\xi,\ \xi_{N+1} = \xi_1 + \zeta$. Suppose we have the following set of states $\{|\psi_n^{\mathrm{ini}}(\xi_j)\rangle,\ j = 1, 2, ..., N, N+1\}$ in an arbitrary gauge (say " ini "),

$$|\psi_n^{\mathrm{ini}}(\xi_1)\rangle,\ |\psi_n^{\mathrm{ini}}(\xi_2)\rangle, ...,\ |\psi_n^{\mathrm{ini}}(\xi_N)\rangle,\ |\psi_n^{\mathrm{ini}}(\xi_{N+1})\rangle. \tag{5}$$

These states may have no special phase relationship. In this case, the Zak phase ϕ_n along a closed loop ($|\psi_n^{\mathrm{ini}}(\xi_1)\rangle \rightarrow |\psi_n^{\mathrm{ini}}(\xi_2)\rangle \rightarrow |\psi_n^{\mathrm{ini}}(\xi_3)\rangle$ ... $|\psi_n^{\mathrm{ini}}(\xi_N)\rangle \rightarrow |\psi_n^{\mathrm{ini}}(\xi_0)\rangle$ with $|\psi_n^{\mathrm{ini}}(\xi_{N+1})\rangle = |\psi_n^{\mathrm{ini}}(\xi_1)\rangle$) is given by [3, 4]

$$\phi_n = -\mathrm{Im}\log[\langle\psi_n^{\mathrm{ini}}(\xi_1)|\psi_n^{\mathrm{ini}}(\xi_2)\rangle\langle\psi_n^{\mathrm{ini}}(\xi_2)|\psi_n^{\mathrm{ini}}(\xi_3)\rangle ... \langle\psi_n^{\mathrm{ini}}(\xi_N)|\psi_n^{\mathrm{ini}}(\xi_1)\rangle]. \tag{6}$$

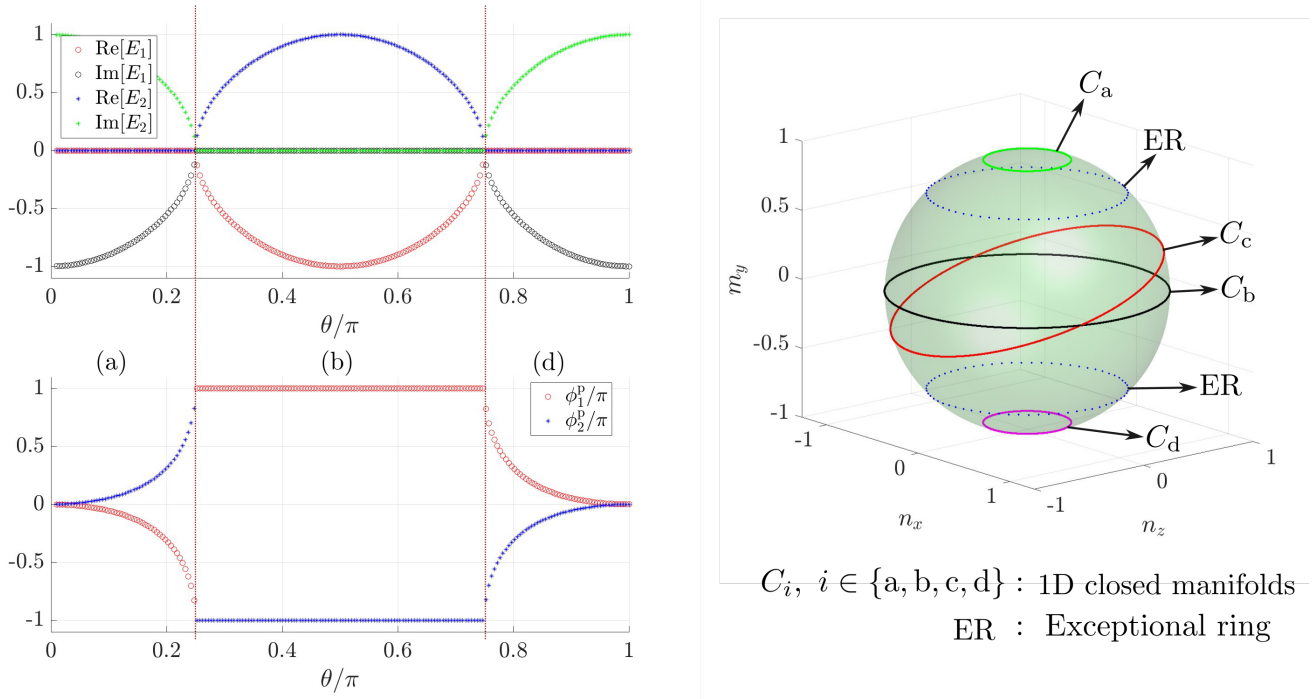

FIG. 1. Left panel (top): Real and Imaginary parts of the eigenvalue spectra as a function of polar angle θ for all values of the azimuthal angle $\Phi \in [0, 2\pi)$. Dotted lines mark the transitions from the $\mathcal{PT}$-exact phase to the $\mathcal{PT}$-broken phase accompanying exceptional points at $\theta = \pi/4, 3\pi/4$ [See Sec. I A]. Left panel (bottom): Zak phases ($\phi^{\rm p}_{n=1,2}$) for two bands as a function of polar angle θ calculated in the parallel transport gauge [See Sec. I B and Sec. I C]. Right panel: Bloch sphere with exceptional rings (marked by ER) and 1D closed manifolds (marked by C_i).

We define a new set of states $\{|\psi^{\rm p}_n(\xi_j)\rangle,\ j = 1, 2, ..., N, N+1\}$ in the *parallel-transport gauge* as follows [3, 4].

$$
\begin{aligned}
|\psi^{\rm p}_n(\xi_1)\rangle &= |\psi^{\rm ini}_n(\xi_1)\rangle, \\
|\psi^{\rm p}_n(\xi_{j+1})\rangle &= e^{i\beta_{j+1}}|\psi^{\rm ini}_n(\xi_{j+1})\rangle,\ \beta_{j+1} = {\rm Im}\log\langle\psi^{\rm p}_n(\xi_{j+1})|\psi^{\rm ini}_n(\xi_j)\rangle,\ j = 1, 2, ..., N.
\end{aligned} \tag{7}
$$

Now, assuming that the states $|\psi^{\rm ini}_n(\xi_{N+1})\rangle = |\psi^{\rm ini}_n(\xi_1)\rangle$. Accordingly, the states $|\psi^{\rm p}_n(\xi_{N+1})\rangle$, $|\psi^{\rm p}_n(\xi_1)\rangle$ also describe the same physical state but may differ by a phase. This phase mismatch is nothing but the Zak phase $\phi^{\rm p}_n = -{\rm Im}\log[\langle\psi^{\rm p}_n(\xi_{N+1})|\psi^{\rm p}_n(\xi_1)\rangle]$[3, 4].

C. Results: Zak phases in $\mathcal{PT}$-exact/broken phases

In this section, we summarize the results of Zak phases calculated using the numerical procedure discussed in the previous section. The behavior of Zak phases for 1D closed manifolds $C = \{\Phi,\ \Phi \in [0, 2\pi)\}$ with constant values of polar angle θ ranging from 0 to π is shown in the bottom panel of Fig. 1. We find that in the parameter regime $\pi/4 < \theta < 3\pi/4$, Zak phases are quantized $|\phi^{\rm p}_{1,2}| = \pi$. However, in the parameter regimes $0 < \theta < \pi/4$ and $\pi/4 < \theta < 2\pi$, Zak phases lose their quantization $|\phi^{\rm p}_{1,2}| \neq \pi$. Moreover, we also find that the quantization of Zak phases does not depend on the orientation of the 1D closed manifolds. For example, Zak phases are the same for closed manifolds $C_{\rm b}$, and $C_{\rm c}$ which have different orientations on the Bloch sphere [See the right panel of Fig. 1].

The quantization of the Zak phase can easily be observed from the amount of discontinuity or phase mismatch of the components of real eigenstates at the end of the closed manifolds in the parallel transport gauge. Therefore, we show the behavior of real and imaginary parts of both components of two right eigenstates along different 1D closed manifolds $C_{\rm a}$, $C_{\rm b}$, $C_{\rm c}$, and $C_{\rm d}$ in the parallel transport gauge in Fig. 2 (a), (b), (c), and (d), respectively.

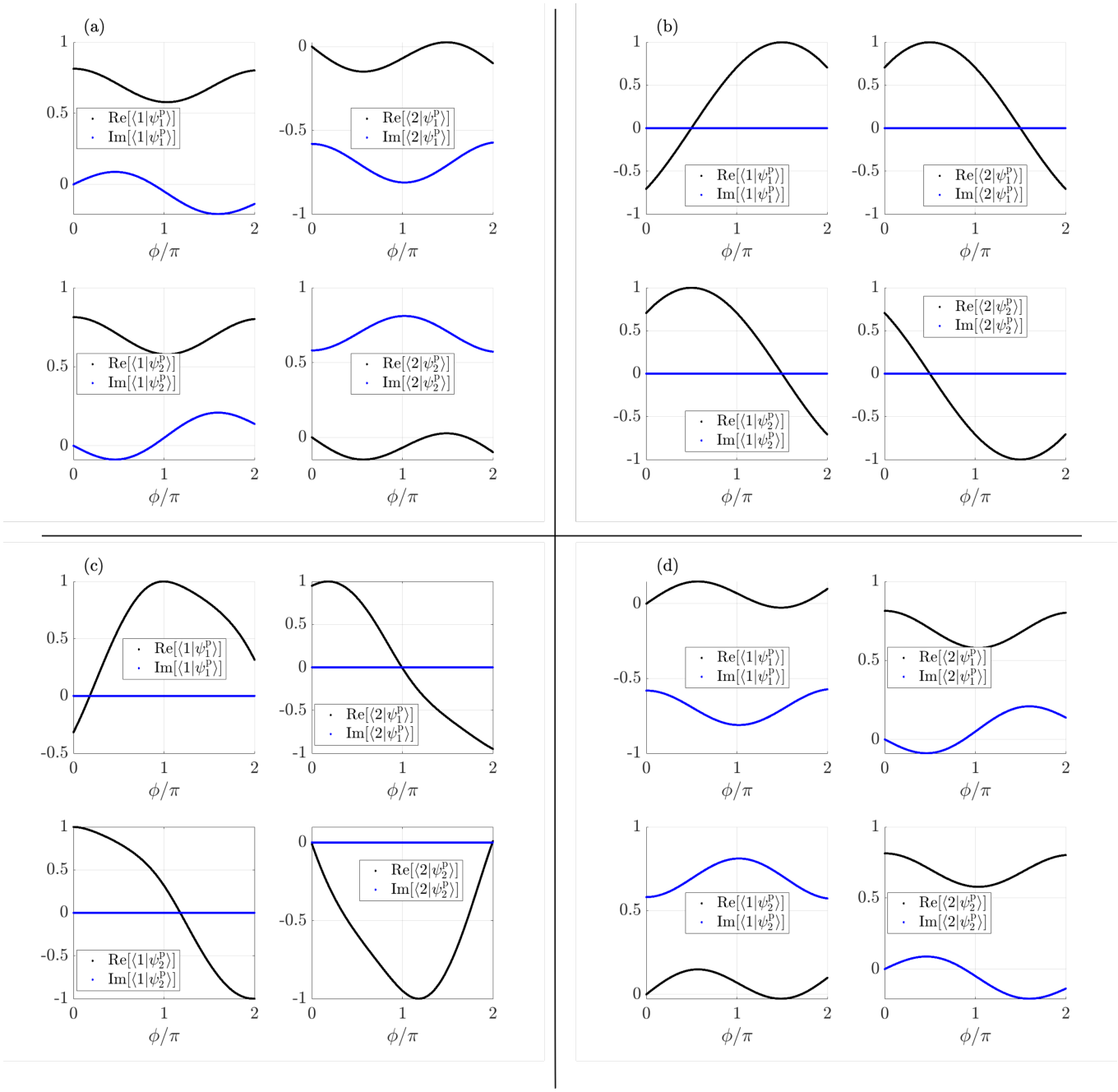

FIG. 2. Parallel transport of eigenstates along different 1D closed manifolds on the Bloch sphere. In (a), (b), (c), and (d), we show the variation of the real and imaginary parts of both the components of the eigenstates for two bands for 1D closed manifolds C_{a}, C_{b}, C_{c}, and C_{d} on the Bloch sphere, respectively [See Sec. I B and the right panel of Fig. 1].

II. FEASIBLE MODEL

In this section, we discuss a more experimentally feasible model of the NHHM. When m_y is set as a small constant, the complexity associated with its momentum dependence is reduced, thus simplifying the implementation in physical systems. The advantage of this scheme is that, even in the presence of small constant value of m_y, the intertwined linking structure of exceptional surfaces is topologically protected and quantization of the Zak phase can still be observed [Fig. 3].

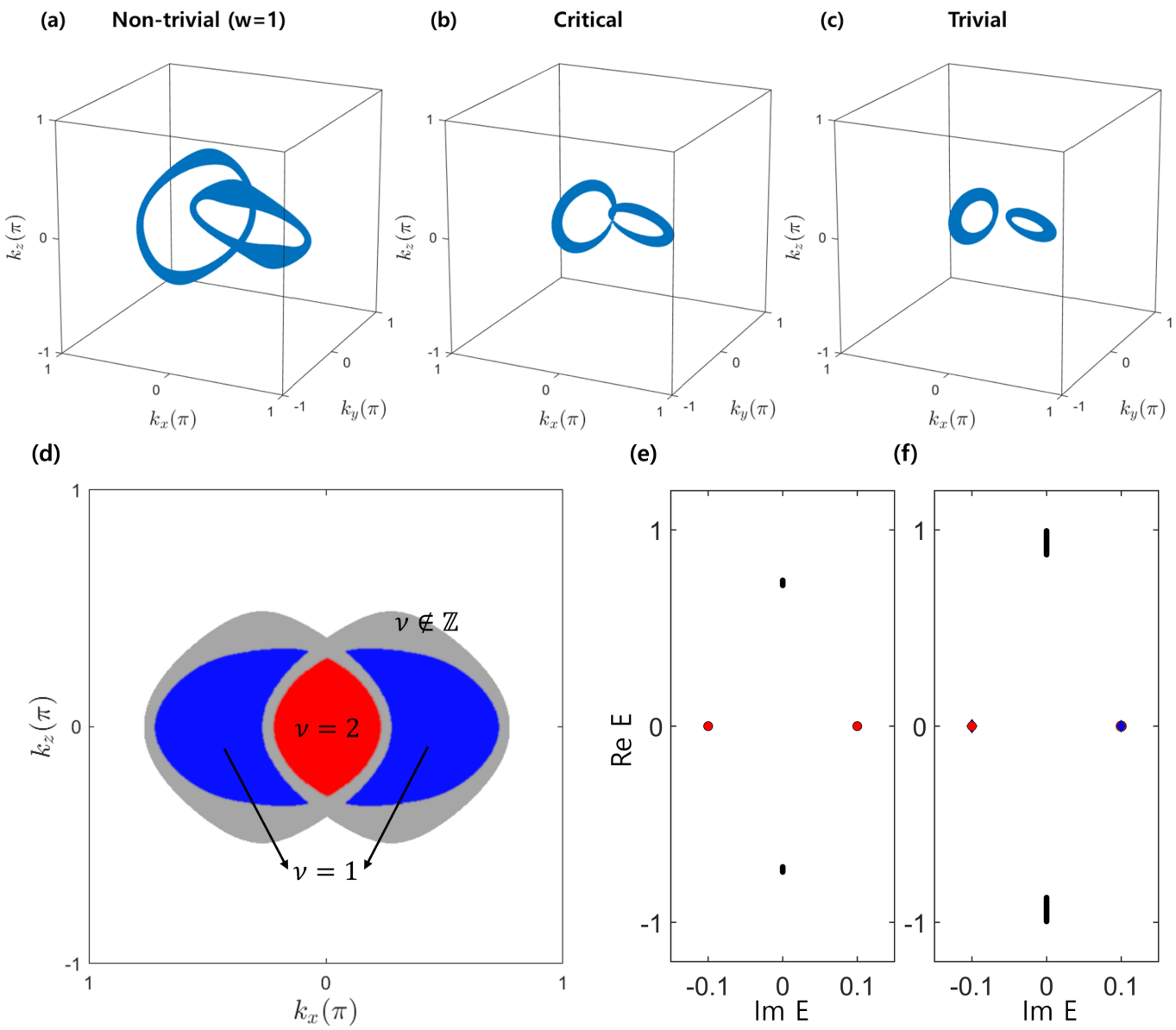

FIG. 3. (a)-(c) The exceptional surfaces in the Brillouin zone when $m_y = 0.1$. (a) Non-trivial value of the Hopf invariant ($w = 1, m = 2$) appears as the linking of the two exceptional surfaces. At the critical point ($m = 3$) (b), the two exceptional surfaces intersect. The two surfaces are completely separated in (c) ($w = 0, m = 3.2$). (d) Illustration of the Zak phase integrated along k_y-direction. Red and blue region has non-trivial Zak phase 2π ($\nu = 2$) and π ($\nu = 1$). Grey region has an ill-defined Zak phase since the line of the integration pass through the exceptional surface. (e)-(f) The eigenenergy spectra in the open boundary condition. Red and blue dots indicate the topological boundary modes, while the black dots represent the bulk spectra. For $\nu = 1$ and $\nu = 2$ loops, (k_x, k_z) are set to $(0.31\pi, 0)$ and $(0.03\pi, 0.03\pi)$, corresponding to blue and red regions in (d), respectively.

[1] M. V. Berry, Quantal Phase Factors Accompanying Adiabatic Changes, Proceedings of the Royal Society of London Series A **392**, 45 (1984).
[2] J. Zak, Berry's phase for energy bands in solids, Phys. Rev. Lett. **62**, 2747 (1989).
[3] A. A. Soluyanov and D. Vanderbilt, Smooth gauge for topological insulators, Phys. Rev. B **85**, 115415 (2012).
[4] D. Vanderbilt, *Berry Phases in Electronic Structure Theory: Electric Polarization, Orbital Magnetization and Topological Insulators* (Cambridge University Press, 2018).

[5] K. Shiozaki, M. Sato, and K. Gomi, Topological crystalline materials: General formulation, module structure, and wallpaper groups, Phys. Rev. B **95**, 235425 (2017).
[6] J. Ahn, D. Kim, Y. Kim, and B.-J. Yang, Band topology and linking structure of nodal line semimetals with Z_2 monopole charges, Phys. Rev. Lett. **121**, 106403 (2018).
[7] J. Ahn, S. Park, D. Kim, Y. Kim, and B.-J. Yang, Stiefel–whitney classes and topological phases in band theory, Chinese Physics B **28**, 117101 (2019).